

Einstein relation for subdiffusive relaxation in Stark chains

P. Prelovšek,¹ S. Nandy,¹ and M. Mierzejewski²

¹*Jožef Stefan Institute, SI-1000 Ljubljana, Slovenia*

²*Institute of Theoretical Physics, Faculty of Fundamental Problems of Technology, Wrocław University of Science and Technology, 50-370 Wrocław, Poland*

(Dated: March 29, 2024)

We investigate chains of interacting spinless fermions subject to a finite external field F (also called Stark chains) and focus on the regime where the charge thermalization follows the subdiffusive hydrodynamics. First, we study reduced models conserving the dipole moment and derive an explicit Einstein relation which links the subdiffusive transport coefficient with the correlations of the dipolar current. This relation explains why the decay rate, Γ_q , of the density modulation with wave-vector q shows q^4 -dependence. In the case of the Stark model, a similar Einstein relation is also derived and tested using various numerical methods. They confirm an exponential reduction of the transport coefficient with increasing F . On the other hand, our study of the Stark model indicates that upon increasing q there is a crossover from subdiffusive behavior, $\Gamma_q \propto q^4$, to the normal diffusive relaxation, $\Gamma_q \propto q^2$, at the wave vector q^* which vanishes for $F \rightarrow 0$.

Introduction. Macroscopic systems driven by finite external forces/fields are usually described within the extended concept of local equilibrium via local thermodynamic parameters as, e.g., the temperature and chemical potential. Such a description can fail when we are dealing with systems isolated from the environment. Prominent recent examples are those of the Stark systems of interacting fermions (which is fermion systems in the presence of a finite field), as realized in tilted cold-atom lattices [1–3]. Such systems reveal several novel theoretical insights and challenges, discussed mostly within one-dimensional (1D) models. Since noninteracting particles subject to a finite external field, F , exhibit Stark localization, the problem shares some similarities with the many-body localization (MBL) (for an overview see [4–7]) and it is known as the Stark MBL [8–18]. It is also well established that effective models, derived at large F from the Stark model (usually by invoking the Schrieffer–Wolff transformations), can exhibit Hilbert space fragmentation [19–24] that violates the eigenstate thermalization hypothesis (ETH) [25–27]. In systems with strongly fragmented Hilbert space, the latter can be linked with the emergence of additional integrals of motion [28, 29].

Still at moderate F , the cold-atom experiments [1] as well as numerical simulations of 1D models [30] reveal the hydrodynamic relaxation of the inhomogeneous particle distributions towards the steady state, which corresponds to the infinite-temperature ($T \rightarrow \infty$) equilibrium. For small wave-vectors $q \ll 1$ the relaxation rates follow a particular subdiffusive (SD) law $\Gamma_q \propto q^4$, rather than the normal diffusive behavior, $\Gamma_q \propto q^2$. This is well consistent with the fact that at $F \neq 0$, the dipole moment emerges in macroscopic systems as an additional conserved quantity [2, 3, 19, 30, 31] and the phenomenological description can be given in terms of the fracton hydrodynamics [31–36]. In spite of a wide consensus that such a description is appropriate for isolated driven systems, so far the theoretical studies are mostly based on

phenomenological hydrodynamic approaches. There are so far very few quantitative results for the subdiffusion in microscopic models [30] as well as theoretical attempts to express the SD transport coefficient D_S [1, 37] in terms of the response functions.

In this Letter, we present the analysis, focused on the particle/density relaxation and anomalous diffusion in the hydrodynamic regime. We consider the standard 1D Stark model, i.e., the chain of interacting spinless fermions subject to a finite external field F , as well as the effective models which involve extended pair-hopping (EPH) interactions and strictly conserve the dipole moment, P . On the one hand, from numerical results for the dynamical density structure factor $S_q(\omega)$, we extract the relaxation rates Γ_q of the density modulation. These rates reveal subdiffusive transport for $q \rightarrow 0$ as well as the value of the corresponding SD coefficient D_S . On the other hand, employing the memory-function (MF) formalism, we derive the Einstein relation that expresses $\Gamma_{q \rightarrow 0}$ in terms of the uniform ($q = 0$) correlations of the normal current, J_N , and the dipolar current, J_D . If P is conserved the response function is determined solely by J_D and the relaxation follows the SD relation $\Gamma_q = D_S q^4$. In the EPH model, J_D is a translationally-invariant operator that governs the relaxation. In the case of the full Stark model, J_D dominates the response for large L (for $F > 0$) when one observes the emergent conservation of the dipole moment. The Einstein relation as well as the numerical results for D_S in both models are tested with alternative numerical approaches. It should be emphasized that the derived Einstein relations remain valid beyond the considered models and even beyond 1D, which we mostly discuss below. Moreover, our numerical results in Stark chains for larger $q > 0$ reveal the crossover from SD $\Gamma_q \sim D_S q^4$ to normal diffusion $\Gamma_q \sim D_N q^2$ at $q \sim q^*(F)$ with vanishing $q^*(F \rightarrow 0)$, consistent with some phenomenological theories [1, 37].

Dynamical density-modulation relaxation. In the fol-

lowing, we study two 1D lattice models of interacting spinless fermions, as they emerge in the presence of the finite external field F , whereby the chain has L sites and open boundary conditions (OBC). The coupling to the field enters the Hamiltonian via $H' = FP$ where P is the dipole moment, $P = \sum_l (l - L/2)n_l$, and n_l is the particle number operator at site l .

Isolated macroscopic Stark systems at finite $F > 0$ develop (heat up) towards a homogeneous steady state $\langle n_l \rangle = \bar{n} = N/L$ (N representing the total particle number), corresponding to $T \rightarrow \infty$ equilibrium. Further on, we analyze dynamics of the periodic density modulation $n_q = \sum_l e^{iql} \tilde{n}_l / \sqrt{L}$, $\tilde{n}_l = n_l - \bar{n}$, and related correlation function $\phi_q(\omega)$,

$$\begin{aligned} \phi_q(\omega) &= \frac{\chi_q(\omega) - \chi_q^0}{\omega} = \frac{-\chi_q^0}{\omega + M_q(\omega)}, \\ \chi_q(\omega) &= \frac{i}{\beta} \int_0^\infty dt e^{i\omega t} \langle [n_{-q}(t), n_q] \rangle, \end{aligned} \quad (1)$$

whereby we define dynamical susceptibilities $\chi_q(\omega)$ and $\chi_q^0 = \chi_q(\omega = 0)$ that remain nonzero even at $\beta = 1/T \rightarrow 0$. In this limit, $\phi_q(\omega)$ is related with the standard dynamical structure factor $S_q(\omega) = \text{Im}\phi_q(\omega)/\pi$. In general, $\phi_q(\omega)$ can be represented in terms of the memory function (MF), $M_q(\omega)$, that determines the profile relaxation rate $\Gamma_q = \text{Im}M_q(\omega = 0)$, which we later on extract also from numerical results for $\phi_q(\omega)$.

Einstein relation. An analytical step towards $M_q(\omega)$ can be made using the MF formalism [38–41], with the introduction of the general scalar product of two operators, $(A|B)$, and the Liouville operator $\mathcal{L}A = [H, A]$. In the case of $\beta \rightarrow 0$, the latter scalar product reduces to thermodynamic average, i.e., $(A|B) \sim \langle A^\dagger B \rangle$. Within this formalism one can express the correlation function as $\phi_q(\omega) = (n_q | (\mathcal{L} - \omega)^{-1} | n_q)$. The memory function can be written in the hydrodynamic regime $q \rightarrow 0$ [39] (in analogy to the perturbation theory [40]) as

$$M_q(\omega) = (\mathcal{L}n_q | (\mathcal{L} - \omega)^{-1} | \mathcal{L}n_q) / \chi_q^0. \quad (2)$$

Expanding n_q in powers of q one obtains,

$$\mathcal{L}n_q \simeq \frac{1}{\sqrt{L}} \left(iq\mathcal{L}P + iq^2 \frac{i}{2} \mathcal{L}Q \right), \quad Q = \sum_l l^2 \tilde{n}_l, \quad (3)$$

where we assumed conservation of the particle number, $\mathcal{L}N = 0$ with $N = \sum_l n_l$. The first term in Eq.(3) represents the normal (uniform) current, $J_N = i\mathcal{L}P$. It determines the hydrodynamic relaxation ($q \rightarrow 0$) in generic systems that do not conserve the dipole moment, $\mathcal{L}P \neq 0$. Namely, one obtains from Eq.(2) the standard Einstein relation [39, 42–44], $\Gamma_q = q^2 \text{Im}\phi_N(0) / \chi_0^0 = D_N q^2$, which links the diffusion constant, D_N , with the current correlation function $\phi_N(\omega) = (J_N | (\mathcal{L} - \omega)^{-1} | J_N) / L$.

If the dipole moment is conserved, $\mathcal{L}P = 0$, then the hydrodynamic relaxation is determined by the second

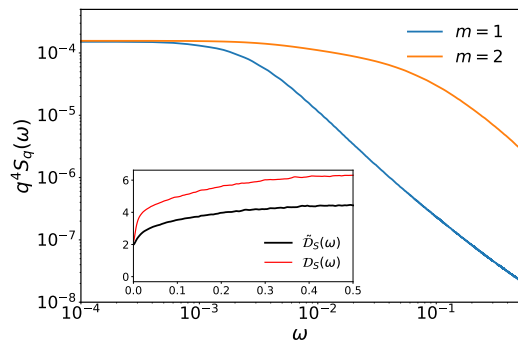


FIG. 1. Dynamical structure factor $q^4 S_q(\omega)$ for the EPH model with $L = 32$ sites, obtained via MCLM for the lowest $q = 2m\pi/L, m = 1, 2$. The inset shows the extracted $\tilde{D}_S(\omega) = \text{Im}M_{q_1}(\omega)/q_1^4$, compared to the Einstein-relation result $D_S(\omega) = \text{Im}\phi_D(\omega)/\chi_0^0$.

term in the expansion in Eq. (3), which can be interpreted as the dipolar current $J_D = \frac{i}{2} \mathcal{L}Q$. Similarly, one then obtains then the Einstein relation $\Gamma_q = D_S q^4$ with $D_S = \text{Im}\phi_D(0)/\chi_0^0$, however, involving the dipolar currents $\phi_D(\omega) = (J_D | (\mathcal{L} - \omega)^{-1} | J_D) / L$. To conclude this part, we note that the MF formalism straightforwardly explains the origin of SD in systems with dipole-moment conservation, $\Gamma_q = D_S q^4$. Similarly to the phenomenological fracton hydrodynamics [31–36], the only assumption we made is the conservation of the dipole moment.

Extended pair-hopping (EPH) model. As a first example we analyze the model where P is strictly a conserved. Starting from the full Stark models, one can derive at $F \gtrsim 1$ the EPH model, either via the Schrieffer-Wolff transformation [19, 20, 31], or expanding the interaction in the Stark basis [28],

$$H_{EPH} = \sum_l \zeta_{dr} [c_{l-r}^\dagger c_l c_{l+d+r}^\dagger c_{l+d} + \text{H.c.}] + H_d. \quad (4)$$

Here, c_l^\dagger, c_l refer to localized Stark states and H_d represents the Hartree-Fock diagonal term, while ζ_{dr} can be derived for given F , at least to lowest order in the interaction [28]. Here, by construction $\mathcal{L}P = 0$. One can derive explicit expression for the dipolar current $J_D = \frac{i}{2} \mathcal{L}Q = \sum_{dr} \zeta_{dr} J_D(d, r)$, where

$$J_D(d, r) = -r(r+d) \sum_j (i c_{j-r}^\dagger c_j c_{j+d+r}^\dagger c_{j+d} + \text{H.c.}). \quad (5)$$

It is remarkable that explicit l -dependence cancels out and J_D emerges as a translationally-invariant operator.

Here, we do not aim to investigate closer the EPH models with realistic parameters, but rather test the existence of SD and the direct expression for the coefficient D_S for a simplified case with $H_d = 0$ and (rather arbitrary) assuming $r = 1$ and values $\zeta_{d1} = 1, 0.75, 0.5, 0.25$ for $d = 1, \dots, 4$. The motivation for including longer-range $d > 1$ terms is that the basic pair-hopping model with

only ζ_{11} is known to exhibit strong Hilbert space fragmentation [19, 20, 22, 23] which invalidates basic ETH concept, while additional terms with $\zeta_{d>1,r>1}$ are expected to suppress this effect [28]. In the following we calculate numerically $\phi_q(\omega)$, Eq. (1), using the micro-canonical Lanczos method (MCLM) for finite L systems [45–47], employing large number of Lanczos steps up to $N_L \sim 10^5$, to achieve the frequency resolution $\delta\omega \lesssim 10^{-4}$ which allows for reliable extraction of $M_q(\omega)$ [47] even for small $q \ll 1$. The advantage of the EPH model (relative to the Stark model) is that in addition to N we use also conservation of P (choosing $P = 0$) to reduce the Hilbert space and to reach $L = 32$ with $N_{st} \sim 10^7$ basis states.

In Fig. 1 we present results for the density structure factor $q^4 S_q(\omega)$ as calculated via MCLM for two lowest $q = q_m = 2m\pi/L, m = 1, 2$. Since we consider the half-filled system $\bar{n} = 1/2$ with effective $T \rightarrow \infty$, we know analytically $\chi_q^0 \sim \chi_0^0 \sim \bar{n}(1 - \bar{n}) = 1/4$. Results confirm very sharp peak at $\omega \sim 0$, being consistent with SD hydrodynamics, i.e., $\pi S_q(\omega \sim 0) \sim \chi_q^0 / \Gamma_q \sim \chi_0^0 / (D_S q^4)$. Moreover, we extract also the corresponding (dynamical) SD coefficient $\bar{D}_S(\omega) = \text{Im} M_q(\omega) / q^4$ for smallest $q = q_1$ and present results in the inset, together with numerically evaluated Einstein relation $D_S(\omega) = \text{Im} \phi_D(\omega) / \chi_0^0$, using J_D from Eq. (5). The agreement is reasonable given that both numerical approaches can suffer from finite-size effects. Moreover, the considered EPH model can still exhibit some features of the Hilbert-space fragmentation [19, 20, 22, 23], which could influence the presumed ETH.

Stark model. We turn further to the properties of the prototype Stark model, i.e., 1D chain of interacting spinless fermions in the presence of a finite external field F ,

$$H = t \sum_i (c_{i+1}^\dagger c_i + c_i^\dagger c_{i+1}) + V \sum_l \tilde{n}_{l+1} \tilde{n}_l + V' \sum_l \tilde{n}_{l+2} \tilde{n}_l + FP, \quad (6)$$

with $\tilde{n}_l = n_l - \bar{n}, n_l = c_l^\dagger c_l$. Fermions interact via the nearest-neighbor (V) and next-nearest-neighbor (V') repulsion. We consider half-filling, i.e., $\bar{n} = N/L = 1/2$, and set $t = 1$ as the unit of energy. We introduce $V' \neq 0$ in order to suppress the integrability (and dissipationless transport) at $F \rightarrow 0$, although the latter effect appears not to be important for $F \gg 0$. In the main text, we restrict the numerical results to the case $V = V' = 1$, while in [48] we discuss also results for $V = 2, V' = 0$.

In the case of the Stark model, Eq. (6), we cannot apply the same analysis as for EPH model, since $\mathcal{L}P \neq 0$ and the conservation of P emerges only in the thermodynamic limit, $L \rightarrow \infty$ [30]. Still, one can derive from Hamiltonian. (6) both contributions to $\mathcal{L}n_q$ in Eq. (3): $J_N = i\mathcal{L}P = \sum_l J_l$ and $J_D = \frac{i}{2}\mathcal{L}Q = J_N/2 + \sum_l l J_l$, where $J_l = itc_l^\dagger c_{l+1} + \text{H.c.}$. Neglecting possible offdiagonal correlations, we can then express the corresponding

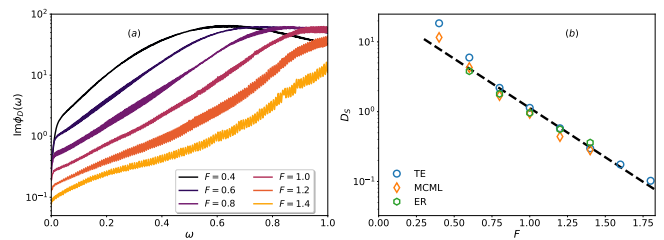


FIG. 2. (a) Dipolar-current correlations $\text{Im} \phi_D(\omega)$ (in log scale) as calculated with MCLM for the Stark model on $L = 28$ sites for different fields F . (b) Subdiffusion coefficient $D_S(F)$, calculated from the rates Γ_{q_1} , obtained via: time-evolution (TE) of the density profile and via MCLM on $L = 24$ chain, and directly from the Einstein relation (ER), i.e., from $\phi_D(\omega)$.

Einstein relation from Eq. (2),

$$M_q(\omega) \simeq [q^2 \phi_N(\omega) + q^4 \phi_D(\omega)] / \chi_0^0. \quad (7)$$

Since in general $\phi_N(\omega) \neq 0$, we can proceed by showing that for finite $F > 0$ and $L \rightarrow \infty$ it follows $\phi_N(\omega \rightarrow 0) = 0$, related to emergent conservation of P [30], as verified also numerically in [48]. Consequently, we expect that at $F > 0$ the hydrodynamic $q \rightarrow 0$ behavior will be dominated by SD with $\Gamma_q = D_S q^4$ with $D_S = \text{Im} \phi_D(\omega \rightarrow 0) / \chi_0^0$.

We further present numerical results for $\text{Im} \phi_D(\omega)$ in Fig. 2(a). Since by construction J_D requires OBC, one cannot guarantee L -independent result for $\phi_D(\omega \rightarrow 0)$. Still, results in Fig. 2(a), obtained with MCLM on $L = 28$ chain, indicate that beyond $F > F_*(L) \gtrsim 0.4$, there is a well defined value $D_S = \text{Im} \phi_D(\omega \rightarrow 0) / \chi_0^0$, revealing already an exponential-like dependence on F . We also note that $\text{Im} \phi_D(\omega)$ for larger ω , as in Fig. 2(a), does not have a direct relation to $M_q(\omega)$, since it neglects $\phi_N(\omega)$ contribution in Eq. (7).

Results for the transport coefficient $D_S(F)$ are summarized in Fig. 2(b). Besides the results from the Einstein relation evaluated via $\phi_D(\omega \rightarrow 0)$ (see Fig. 2(a)), we include also results for $D_S = \Gamma_q / q^4$ obtained from two alternative approaches applied for $L = 24$ chain and the smallest $q_1 = 2\pi/L$. Namely, we extract Γ_q directly from the MCLM results for $S(q, \omega \rightarrow 0)$, as well as from the decay of the inhomogeneous density profile where F is introduced via the time-dependent flux [30, 49]. The latter method evaluates the relaxation rate Γ_q (see [50] for the details), with the advantage of periodic boundary conditions and consequently resolving also very small D_S , i.e., reaching larger $F \simeq 2$. Results in Fig. 2(b) are quantitatively consistent in the broad regime of $F > F_*(L) \sim 0.4$, confirming the validity of the Einstein relation for SD transport as well as the exponential dependence of $D_S(F)$. In [48] we present results also for other parameters, in particular for $V = 2, V' = 0$, where we employ also the boundary-driven open systems

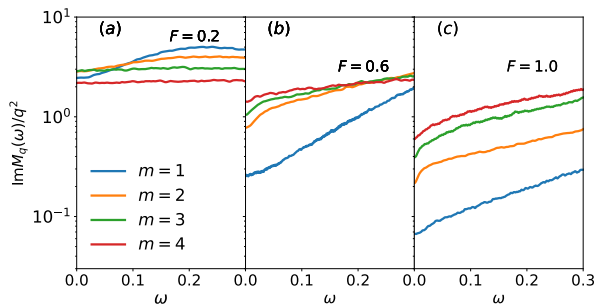


FIG. 3. Dynamical relaxation rates $\Gamma_q(\omega)/q^2$ (in log scale), as extracted from MCLM results for $\phi_q(\omega)$ on $L = 24$ chain and $q_m = 2m\pi/L$, $m = 1 - 4$, for three different regimes of F .

[30, 50], allowing for the analysis of considerably larger $L \leq 50$ as well as the direct evaluation of D_S via the form of the nonequilibrium stationary density profile [48].

Crossover to normal diffusion. Let us finally examine closer $M_q(\omega)$ at larger q as extracted numerically from $\phi_q(\omega)$, again for parameters $V = V' = 1$. Fig. 3 shows MCLM results for $\text{Im}M_q(\omega)/q^2$ obtained for various $q = 2m\pi/L$ with $1 \leq m \leq 4$ and $L = 24$ so that $q \leq \pi/3$. One can resolve three regimes. Despite finite-size limitations, results at small $F = 0.2 < F_*(L)$, shown in Fig. 3(a), are approximately consistent with normal diffusion for all presented q_m , i.e., $\text{Im}M_q(\omega) \propto q^2$. At intermediate $F_*(L) < F < F_c \sim 1$, as in Fig. 3(b), only the smallest $q = q_1$ evidently deviates, the latter being the signature of the SD transport $\text{Im}M_q(\omega \sim 0) \propto q^4$. Still, the relaxation functions $\text{Im}M_q(\omega)/q^2$ nearly overlap for larger q which can be interpreted as an effective normal diffusion $\text{Im}M_q(\omega) \propto q^2$. Finally, for large $F \gtrsim F_c$, as in Fig. 3(c), an anomalous SD-like relaxation appears for all $q < 1$.

In Fig. 4(a) we collect results for an effective normal diffusion coefficient $\tilde{D}_N = \text{Im}M_q(\omega = 0)/q^2$ at largest $q = q_4 = \pi/3$ as in Fig. 3. Taking results for D_S from Fig. 2(b) and \tilde{D}_N from Fig. 4(a) one may estimate that the crossover between SD and diffusive relaxations is expected at the wavevector q^* fulfilling the relation $D_S(q^*)^4 = \tilde{D}_N(q^*)^2$. Numerical results from such estimate are shown in Fig. 4(b), representing a rough phase diagram of normal-SD transport, relevant at least for moderate $F < F_c$. While we expect a continuous vanishing of q^* for $F \rightarrow 0$, it is hard to numerically determine the dependence $q^*(F \ll 1)$ due to finite-size limitations. Still, the general trend of $q^*(F)$ is well consistent with phenomenological approaches [1, 37]. We should also note that the explicit MF expression, Eq. (7), is restricted only to the hydrodynamic regime $q \rightarrow 0$ when $M_q(\omega)$ is small and $\phi_N(\omega \rightarrow 0)$ strictly vanishes. Therefore, it cannot be extended to the discussion of the normal/SD crossover at larger q .

Conclusions. In this Letter, we present the analysis

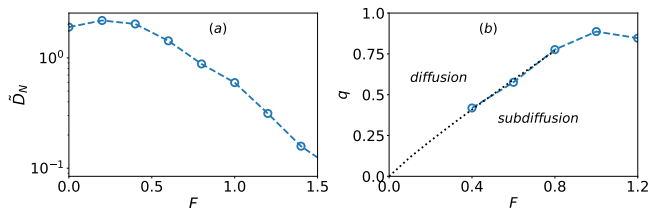


FIG. 4. (a) Effective normal diffusion coefficient $\tilde{D}_N = \Gamma_q/q^2$ for $q = \pi/3$ vs. F , evaluated at $q = \pi/3$ via MCLM on $L = 24$ sites. (b) Effective phase diagram $q^*(F)$ with the SD/normal diffusion crossover at $q^*(F)$, with the dotted line representing the qualitative guess for small F .

of the Stark models, based on the memory-function approach to hydrodynamics. It enables a direct consideration of the subdiffusion and the corresponding transport coefficient D_S . In models with strictly conserved dipole moment P , the derivation yields a subdiffusive relaxation rates, $\Gamma_q = D_S q^4$ and an explicit Einstein relation which links D_S with correlations of the uniform ($q = 0$) dipolar current J_D . In the full Stark problem, where P is conserved only in the thermodynamic limit, the analogous treatment is valid only in more restricted hydrodynamic regime $q \rightarrow 0$. However, the correlations of the dipolar current are still linked with D_S via the Einstein relation. Moreover, the obtained numerical results agree with alternative numerical approaches, at least in the range of F where the finite-size limitations allow for reliable numerical studies. As a general observation, we note that the coefficient D_S reveals a strong exponential-like reduction with F , which for large $F \gg 1$ can effectively appear as Stark MBL concept [8–18], as well as the Hilbert-space fragmentation [19–24]. It should be stressed that the presented Einstein relations are not specific to considered model and even not to one-dimensional systems. They can be easily generalized to models which are more relevant for experiments as, e.g., the tilted Fermi-Hubbard model.

We acknowledge the support by Slovenian Research and Innovation Agency (ARIS) via the program P1-0044 (P.P., S.N.) and the project J1-2463 (S.N.) as well as the National Science Centre, Poland via project 2020/37/B/ST3/00020 (M.M.). S. N. acknowledges also the EU support via QuantERA grant T-NiSQ, and also computing time at the supercomputer Vega at IZUM, Slovenia. The numerical calculation were partly carried out at the facilities of the Wroclaw Centre for Networking and Supercomputing. Our TEBD code was written using ITensors Library in Julia [51].

[1] E. Guardado-Sanchez, A. Morningstar, B. M. Spar, P. T. Brown, D. A. Huse, and W. S. Bakr, Subdiffusion

- and heat transport in a tilted two-dimensional Fermi-Hubbard system, *Phys. Rev. X* **10**, 011042 (2020).
- [2] S. Scherg, T. Kohlert, P. Sala, F. Pollmann, B. Hebbe Madhusudhana, I. Bloch, and M. Aidelsburger, Observing non-ergodicity due to kinetic constraints in tilted Fermi-Hubbard chains, *Nature Communications* **12**, 4490 (2021).
 - [3] T. Kohlert, S. Scherg, P. Sala, F. Pollmann, B. Hebbe Madhusudhana, I. Bloch, and M. Aidelsburger, Exploring the regime of fragmentation in strongly tilted Fermi-Hubbard chains, *Phys. Rev. Lett.* **130**, 010201 (2023).
 - [4] R. Nandkishore and D. A. Huse, Many-body localization and thermalization in quantum statistical mechanics, *Annual Review of Condensed Matter Physics* **6**, 15 (2015).
 - [5] F. Alet and N. Laflorencie, Many-body localization: An introduction and selected topics, *Comptes Rendus. Physique* **19**, 498 (2018).
 - [6] D. A. Abanin, E. Altman, I. Bloch, and M. Serbyn, Colloquium: Many-body localization, thermalization, and entanglement, *Rev. Mod. Phys.* **91**, 021001 (2019).
 - [7] P. Sierant, M. Lewenstein, A. Scardicchio, L. Vidmar, and J. Zakrzewski, Many-body localization in the age of classical computing (2024), [arXiv:2403.07111 \[cond-mat.dis-nn\]](https://arxiv.org/abs/2403.07111).
 - [8] M. Schulz, C. A. Hooley, R. Moessner, and F. Pollmann, Stark many-body localization, *Phys. Rev. Lett.* **122**, 040606 (2019).
 - [9] E. Nieuwenburg, Y. Baum, and G. Rafael, From Bloch oscillations to many-body localization in clean interacting systems, *Proceedings of the National Academy of Sciences of the United States of America* **116**, 9269 (2019).
 - [10] S. R. Taylor, M. Schulz, F. Pollmann, and R. Moessner, Experimental probes of Stark many-body localization, *Phys. Rev. B* **102**, 054206 (2020).
 - [11] D. S. Bhakuni, R. Nehra, and A. Sharma, Drive-induced many-body localization and coherent destruction of Stark many-body localization, *Phys. Rev. B* **102**, 024201 (2020).
 - [12] L. Zhang, Y. Ke, W. Liu, and C. Lee, Mobility edge of Stark many-body localization, *Phys. Rev. A* **103**, 023323 (2021).
 - [13] W. Morong, F. Liu, P. Becker, K. S. Collins, L. Feng, A. Kyprianidis, G. Pagano, T. You, A. V. Gorshkov, and C. Monroe, Observation of Stark many-body localization without disorder, *Nature* **599**, 393 (2021).
 - [14] Y.-Y. Wang, Z.-H. Sun, and H. Fan, Stark many-body localization transitions in superconducting circuits, *Phys. Rev. B* **104**, 205122 (2021).
 - [15] E. V. H. Doggen, I. V. Gornyi, and D. G. Polyakov, Stark many-body localization: Evidence for Hilbert-space shattering, *Phys. Rev. B* **103**, L100202 (2021).
 - [16] T. M. Gunawardana and B. Buča, Dynamical l-bits and persistent oscillations in Stark many-body localization, *Phys. Rev. B* **106**, L161111 (2022).
 - [17] G. Zisling, D. M. Kennes, and Y. Bar Lev, Transport in Stark many-body localized systems, *Phys. Rev. B* **105**, L140201 (2022).
 - [18] X. Wei, X. Gao, and W. Zhu, Static and dynamical Stark many-body localization transition in a linear potential, *Phys. Rev. B* **106**, 134207 (2022).
 - [19] P. Sala, T. Rakovszky, R. Verresen, M. Knap, and F. Pollmann, Ergodicity breaking arising from Hilbert space fragmentation in dipole-conserving Hamiltonians, *Phys. Rev. X* **10**, 011047 (2020).
 - [20] V. Khemani, M. Hermele, and R. Nandkishore, Localization from Hilbert space shattering: From theory to physical realizations, *Phys. Rev. B* **101**, 174204 (2020).
 - [21] Z.-C. Yang, F. Liu, A. V. Gorshkov, and T. Iadecola, Hilbert-space fragmentation from strict confinement, *Phys. Rev. Lett.* **124**, 207602 (2020).
 - [22] S. Moudgalya and O. I. Motrunich, Hilbert space fragmentation and commutant algebras, *Phys. Rev. X* **12**, 011050 (2022).
 - [23] S. Moudgalya, B. A. Bernevig, and N. Regnault, Quantum many-body scars and Hilbert space fragmentation: a review of exact results, *Reports on Progress in Physics* **85**, 086501 (2022).
 - [24] X. Feng and B. Skinner, Hilbert space fragmentation produces an effective attraction between fractons, *Phys. Rev. Res.* **4**, 013053 (2022).
 - [25] J. M. Deutsch, Quantum statistical mechanics in a closed system, *Phys. Rev. A* **43**, 2046 (1991).
 - [26] M. Srednicki, Chaos and quantum thermalization, *Phys. Rev. E* **50**, 888 (1994).
 - [27] L. D'Alessio, Y. Kafri, A. Polkovnikov, and M. Rigol, From quantum chaos and eigenstate thermalization to statistical mechanics and thermodynamics, *Advances in Physics* **65**, 239 (2016), 1509.06411.
 - [28] P. Lydzba, P. Prelovšek, and M. Mierzejewski, Local integrals of motion in dipole-conserving models with Hilbert space fragmentation, (2024), [arXiv:2401.17097 \[cond-mat.str-el\]](https://arxiv.org/abs/2401.17097).
 - [29] T. Rakovszky, P. Sala, R. Verresen, M. Knap, and F. Pollmann, Statistical localization: From strong fragmentation to strong edge modes, *Phys. Rev. B* **101**, 125126 (2020).
 - [30] S. Nandy, Z. Lenarčič, E. Ilievski, M. Mierzejewski, J. Herbrych, and P. Prelovšek, Spin diffusion in a perturbed isotropic Heisenberg spin chain, *Phys. Rev. B* **108**, L081115 (2023).
 - [31] J. Feldmeier, P. Sala, G. De Tomasi, F. Pollmann, and M. Knap, Anomalous diffusion in dipole- and higher-moment-conserving systems, *Phys. Rev. Lett.* **125**, 245303 (2020).
 - [32] R. M. Nandkishore and M. Hermele, Fractons, *Annual Review of Condensed Matter Physics* **10**, 295 (2019).
 - [33] A. Gromov, A. Lucas, and R. M. Nandkishore, Fracton hydrodynamics, *Phys. Rev. Res.* **2**, 033124 (2020).
 - [34] A. G. Burchards, J. Feldmeier, A. Schuckert, and M. Knap, Coupled hydrodynamics in dipole-conserving quantum systems, *Phys. Rev. B* **105**, 205127 (2022).
 - [35] J. Guo, P. Glorioso, and A. Lucas, Fracton hydrodynamics without time-reversal symmetry, *Phys. Rev. Lett.* **129**, 150603 (2022).
 - [36] A. Głodkowski, F. Peña Benítez, and P. Surówka, Hydrodynamics of dipole-conserving fluids, *Phys. Rev. E* **107**, 034142 (2023).
 - [37] P. Zechmann, A. Bastianello, and M. Knap, Tunable transport in the mass-imbalanced Fermi-Hubbard model, *Phys. Rev. B* **106**, 1 (2022), 2205.12970.
 - [38] H. Mori, Transport, collective motion, and Brownian motion, *Progress in Theoretical Physics* **33**, 423 (1965).
 - [39] D. Forster, *Hydrodynamic Fluctuations, Broken Symmetry and Correlation Functions*, Taylor - Francis Group, CRC Press (1975).
 - [40] W. Götze and P. Wölfle, Homogeneous dynamical conductivity of simple metals, *Phys. Rev. B* **6**, 1226 (1972).

- [41] P. Jung and A. Rosch, Lower bounds for the conductivities of correlated quantum systems, *Phys. Rev. B* **75**, 245104 (2007).
- [42] L. P. Kadanoff and P. C. Martin, Hydrodynamic equations and correlation functions, *Annals of Physics* **24**, 419 (1963).
- [43] J. Bonča and J. Jaklič, Spin diffusion of the t-J model, *Phys. Rev. B* **51**, 16083 (1995).
- [44] R. Steinigeweg and J. Gemmer, Density dynamics in translationally invariant spin-1/2 chains at high temperatures: A current-autocorrelation approach to finite time and length scales, *Phys. Rev. B* **80**, 40 (2009).
- [45] M. W. Long, P. Prelovšek, S. El Shawish, J. Karadamoglou, and X. Zotos, Finite-temperature dynamical correlations using the microcanonical ensemble and the Lanczos algorithm, *Phys. Rev. B* **68**, 235106 (2003).
- [46] P. Prelovšek and J. Bonča, Ground state and finite temperature Lanczos methods, in *Strongly Correlated Systems - Numerical Methods*, edited by A. Avella and F. Mancini (Springer, Berlin, 2013).
- [47] J. Herbrych, R. Steinigeweg, and P. Prelovšek, Spin hydrodynamics in the $s = \frac{1}{2}$ anisotropic Heisenberg chain, *Phys. Rev. B* **86**, 115106 (2012).
- [48] See Supplemental Material for the analysis the relaxation of dipole moment and related current correlations, as well as for results for other model parameters, involving also the additional numerical approach using the boundary-driven open systems.
- [49] M. Mierzejewski and P. Prelovšek, Nonlinear current response of an isolated system of interacting fermions, *Phys. Rev. Lett.* **105**, 1 (2010).
- [50] S. Nandy, J. Herbrych, Z. Lenarčič, A. Głódkowski, P. Prelovšek, and M. Mierzejewski, Emergent dipole moment conservation and subdiffusion in tilted chains, *Phys. Rev. B* **109**, 115120 (2024).
- [51] M. Fishman, S. R. White, and E. M. Stoudenmire, The ITensor Software Library for Tensor Network Calculations, *SciPost Phys. Codebases*, 4 (2022).
- [52] P. Prelovšek, S. Nandy, Z. Lenarčič, M. Mierzejewski, and J. Herbrych, From dissipationless to normal diffusion in the easy-axis Heisenberg spin chain, *Phys. Rev. B* **106**, 245104 (2022).

Supplemental Material: Einstein relation for subdiffusive relaxation in Stark chains

P. Prelovšek¹, S. Nandy¹, M. Mierzejewski²

¹*Department of Theoretical Physics, J. Stefan Institute, SI-1000 Ljubljana, Slovenia*

²*Institute of Theoretical Physics, Faculty of Fundamental Problems of Technology,
Wrocław University of Science and Technology, 50-370 Wrocław, Poland*

In the Supplemental Material we analyze the relaxation of dipole moment and related current correlations, We present also results for other model parameters, involving the additional numerical approach using the boundary-driven open systems.

RELAXATION OF THE DIPOLE MOMENT AND CURRENT CORRELATIONS

Studying the Stark chain in the main text we argue that for large L , nonzero F and small ω , the dominating contribution to the memory function, Eq. (7), comes from the dipolar currents, $\phi_D(\omega)$, instead of the normal current correlations, $\phi_N(\omega)$. The latter expectation originates from the emergent conservation of the dipole moment in macroscopic systems, $L \rightarrow \infty$ [50]. Below we provide numerical results which support this claim. However, we note that in a finite system one gets $\phi_N(\omega = 0) = 0$ just due to open boundary conditions (OBC) simply because a finite system with OBC cannot host a steady current. In order to disentangle the influence of OBC in a finite system from the conservation of the dipole moment we study the relaxation of the dipole moment $P = \sum_l (l - L/2)n_l$. To this end we calculate the correlation function

$$\phi_P(\omega) = \langle P | (\mathcal{L} - \omega)^{-1} | P \rangle = \frac{-\chi_P^0}{\omega + N(\omega)}. \quad (\text{S1})$$

In equation (S1) we introduced the corresponding MF

$$N(\omega) = \frac{L}{\chi_P^0} \tilde{\phi}_N(\omega), \quad (\text{S2})$$

where $\chi_P^0 = \langle P^2 \rangle$ and formally MF can be expressed as [39],

$$\tilde{\phi}_N(\omega) = (\mathcal{L}P | (\tilde{\mathcal{L}} - \omega)^{-1} | \mathcal{L}P) / L = (J_N | (\tilde{\mathcal{L}} - \omega)^{-1} | J_N) / L, \quad (\text{S3})$$

where we used the identity $\mathcal{L}P = -iJ_N$. In contrast to Eq. (2) in the main text that is valid in the hydrodynamic (perturbative) regime, there is no small parameter in Eq. (S3) thus $\tilde{\mathcal{L}}$ contains additional projectors [39],

$$\tilde{\mathcal{L}} = \mathcal{Q}\mathcal{L}\mathcal{Q}, \quad \mathcal{Q} = 1 - \mathcal{P}, \quad \mathcal{P} = \frac{|P\rangle\langle P|}{\langle P|P\rangle}. \quad (\text{S4})$$

For this reason in a finite system $\tilde{\phi}_N(\omega)$ in Eq. (S3) is not equal to $\phi_N(\omega) = (J_N | (\mathcal{L} - \omega)^{-1} | J_N) / L$ but both quantities should merge for $L \rightarrow \infty$ due to the conservation of P .

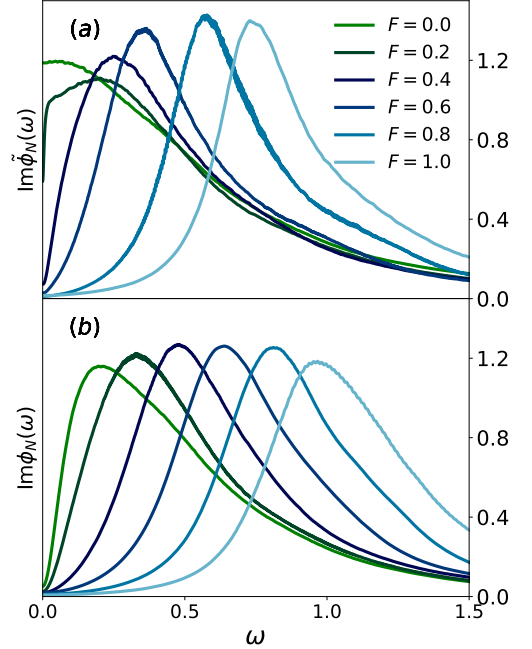


FIG. S1. (a) The current correlation function $\text{Im}\tilde{\phi}_N(\omega)$, as extracted from dipole-moment correlations $\phi_P(\omega)$, calculated for Stark model using MCLM on $L = 28$ chain, for different fields $F = 0 - 1.0$, (b) directly evaluated current correlations $\text{Im}\phi_N(\omega)$ in the same system.

Due to the presence of projectors, it is hard to determine $\tilde{\phi}_N(\omega)$ from Eq. (S3). However, this quantity can be obtained also from the correlations of the dipole moment via Eqs. (S1) and (S2). In order to confirm the relation between $\tilde{\phi}_N(\omega)$ and $\phi_N(\omega)$ and related conjectures, we numerically investigate the Stark model with the same parameters $V = V' = 1$ for different fields $F \leq 1$. On one hand, using MCLM on the $L = 28$ system with OBC, we evaluate $\phi_P(\omega)$ and extract the corresponding $\text{Im}\tilde{\phi}_N(\omega)$. On the other hand, we calculate within the same system directly $\text{Im}\phi_N(\omega)$. Numerical results presented in Figs. S1(a) and S1(b) confirm that at $F > F^* \sim 0.4$ (for considered $L = 28$) both approaches

indeed yield (at least qualitatively) $\tilde{\phi}_N(\omega) \sim \phi_N(\omega)$, up to finite-size effects. As expected, the disagreement occurs at $F \sim 0$ since $\phi_N(\omega \rightarrow 0)$ vanishes due to OBC, while $\tilde{\phi}_N(\omega \rightarrow 0)$ does not. Due to the same argument the qualitative discrepancy in the range $F < F^*(L)$ can be attributed to finite-size limitations.

The main conclusion is that P behaves as a conserved quantity and, at the same time, $\text{Im}\phi_N(\omega \rightarrow 0) \rightarrow 0$, so that in Eq. (7) in the main text one can neglect the latter contribution in the hydrodynamic regime $q \rightarrow 0$. Consequently, the relaxation is then dominated by the SD contribution, i.e., $M_q(\omega \sim 0) \sim q^4 \phi_D(\omega \rightarrow 0)/\chi_0^0$. Based on results in Fig. S1 this conclusion holds true at least for $F > F^* \sim 0.4$, whereby we expect that F^* vanishes in the thermodynamic limit.

SUBDIFFUSION COEFFICIENT FROM BOUNDARY DRIVEN OPEN SYSTEMS

As an additional technique to compute the subdiffusion constant, we study an open chain described by Eq. (6), driven via boundary Lindblads operators inducing a weak particle current by creating a bias μ at the edges of the system. The master equation governing the time-evolution of the density matrix is given by

$$\partial_t \rho = -i[H, \rho] + \hat{D}\rho \quad (\text{S5})$$

where \hat{D} denotes the dissipator operator written in terms of the Lindblads as $\hat{D}\rho = \sum_k L_k \rho L_k^\dagger - \frac{1}{2}\{L_k^\dagger L_k, \rho\}$. The details of the Lindblads employed here are discussed in [30, 50, 52]. To evolve the density matrix towards the steady state ρ_{ss} , we use the time-evolving block decimation (TEBD) for vectorized density matrices. In particular, we use the fourth-order TEBD with a time step $dt = 0.2$, bond dimension $\chi \sim 140$, and weak bias $\mu = 0.01$.

The method allows us to establish a nonequilibrium steady state (NESS) for which the normalized current I/μ and the spatial profile of particles $\langle \tilde{n}_i \rangle$ can be easily computed. One remarkable advantage of this technique is that the NESS profile carries the signature of the nature of particle transport [50]. In particular, for system with both particle-number and dipole-moment conservation, the hydrodynamic equation of motion $\partial_t n + D\partial_x^4 n = 0$ implies the NESS particle profile of the form $\langle \tilde{n}_i \rangle = ax + bx^3, x = 2\ell/L - 1$.

We further present and analyse the NESS results for the case $V = 2, V' = 0$, which is at $F = 0$ equivalent to the isotropic Heisenberg model with the corresponding particle superdiffusion [30], while for $F > 0$ the SD is expected with results similar as presented in the main text for $V = V' = 1$. Fig. S2 clearly demonstrates how the normalized particle profile changes with increasing F . The profile at $F = 0$ is indeed a signature of particle superdiffusion where $\langle \tilde{n}_i \rangle \sim \arcsin(x)$ (see [30] for

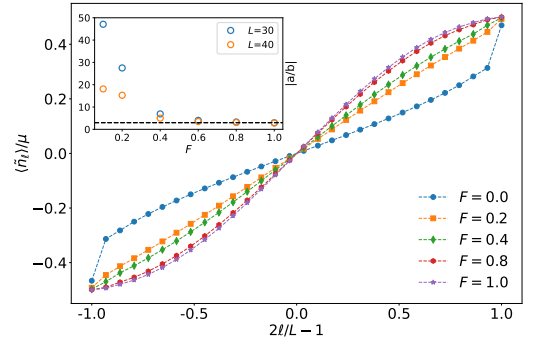


FIG. S2. Steady-state density profiles $\langle \tilde{n}_i \rangle / \mu$ obtained by the boundary-driven open-system approach, obtained for different fields F on $L = 40$ system. Inset shows the ratio of profile coefficients $|a/b|$ vs. F for two system sizes L .

details). As evident in Fig. S2, increasing $F > 0$ leads to qualitative change of the profile. Whereas it is close to linear (corresponding to normal diffusion) for small finite $F \lesssim 0.4$, eventually the profile becomes cubic for larger $F \gtrsim 0.6$, being a direct signature of the crossover to SD transport. Here, we refer to reference [50], for further details regarding the fitting of coefficients a, b . Finally, for large F with the SD transport we establish the ratio $|a/b| \sim 3$, as the consequence of vanishing derivative $\delta_x(ax + bx^3)|_{x=\pm 1} = 0$ at the edges, being evident in the main panel of Fig. S3. The inset shows that indeed the ratio $|a/b| \rightarrow 3$ with increasing F and also with increasing L . We argue that the edge flatness carries the signature of the fact that in SD systems the normal current becomes zero (or negligibly small) for $F > 0$ in the $L \rightarrow \infty$ limit. Using the relation $|a/b| = 3$, the SD coefficient can be then expressed directly with the obtained NESS current as $D_S = IL^3/(12\mu)$.

RESULTS FOR OTHER MODEL PARAMETERS

We present in Fig. S3 the summary of results for the SD coefficient D_S , as obtained by different numerical approaches for parameters $V = 2, V' = 0$, corresponding to the isotropic Heisenberg model subject to constant field (magnetic field gradient). Besides the methods presented and used in the main text, i.e., the time-evolution (TE) and MCLM where D_S is extracted from relaxation rates $D_S = \Gamma_{q_1}/q_1^4$ for the smallest $q_1 = 2\pi/L$ at $L = 24$, and the direct evaluation using the Einstein relation (ER) on $L = 28$ chain, we include now also the NESS results for the boundary-driven systems with $L \lesssim 50$. Results are presented for fields $F > F^*(L) \sim 0.4$ where the SD transport is dominant for numerically accessible L . Employed methods have also different numerical limitations at large $F > 1$. While the NESS approach is limited by smallness of the current I , the MCLM and Einstein

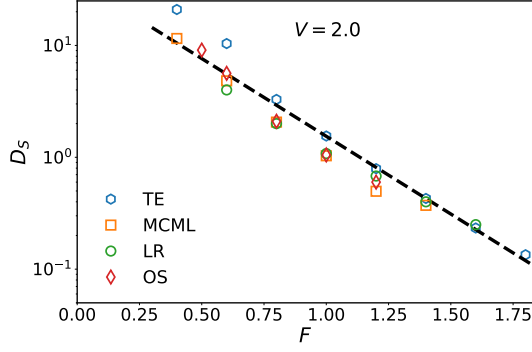


FIG. S3. Subdiffusion coefficient $D_S(F)$, as calculated: from rates Γ_{q_1} , obtained via time-evolution (TE) and via MCLM on $L = 24$ chain, and directly from Einstein relation (ER) and $\phi_D(\omega)$ on $L = 28$ chain, as well via the boundary-driven open systems (OS) on $L \leq 50$ chains.

relation are limited by the frequency resolution and the influence of OBC, so the time-evolution approach has the advantage of smallest reachable Γ_q and consequently of largest reachable $F \lesssim 2$ due to PBC in this case. The overall conclusion following from Fig. S3 is that results by different methods are even quantitatively well consistent, revealing again the strong/exponential dependence of D_S on F . On the other hand, by comparing with Fig. 2 (b) in the main text, we also notice that D_S only weakly depends on the interaction parameters V and V' . For stronger interactions we observe an increase D_S at larger F since the interaction suppresses localization, while at weaker F the trend might be opposite, but further studies are needed to establish such relations.